Eur. Phys. J. B (2022)95:87
https://doi.org/10.1140/epjb/s10051-022-00352-7

THE EUROPEAN PHYSICAL JOURNAL B

Regular Article - Solid State and Materials

A generalized Frenkel–Kontorova model for a propagating austenite–martensite phase boundary: revisited numerically

W. Quapp[1,a] and J. M. Bofill[2,b]

[1] Mathematisches Institut, Universität Leipzig, PF 100920, 04009 Leipzig, Germany
[2] Departament de Química Inorgànica i Orgànica, Secció de Química Orgànica, and Institut de Química Teòrica i Computacional, (IQTCUB), Universitat de Barcelona, Martí i Franquès 1, 08028 Barcelona, Spain

Received 27 January 2022 / Accepted 12 May 2022

Abstract. We explain the propagating austenite–martensite phase boundary by a Frenkel–Kontorova model for a chain of meshes along a ledge of the phase transitions. We demonstrate such steps for example chains of 16 and 47 meshes. We can represent a Langevin solution which describes possible cases of a consecutive excitation of a higher phase under a low external force.

1 Introduction

Shape memory alloys (SMAs) are interesting for applications by two properties: the shape memory effect and the pseudoelasticity. SMAs are able to recover strain due to their phase transformation between austenite (Au) and martensite (Ma). One example is the nearly equiatomic nickel–titanium alloy [1,2]. The wide use of SMAs in engineering applications requires a deeper understanding of these materials.

This paper is inspired by the work of Leninpadian and Vedantam [3] where the propagation of an Au–Ma phase boundary is explained by the help of a generalized Frenkel–Kontorova (FK) model [4]. Compare the corresponding Figure 2 in [3]. Though the martensite phase is connected with a lower temperature, the austenite phase can 'relax' to the higher energy under an external force. In contrast to Ref. [3] we describe a consecutive phase transition through the full ledge of meshes. The model is explained in Sects. 2 and 3.

An FK model was also proposed for crack tip instabilities in [5], and in many other works—sometimes without to name it so. To look inside the FK chain we use in this work the potential energy surface (PES) of a chain of meshes [6–9]. The PES maps possible configurations of the chain to their corresponding energy. Of special interest is always a low-lying pathway, a valley, which connects different stationary structures. The neighbourhood of such a pathway is the way where the FK chain can move under a mild external force, if it could be depinned before.

In contrast to the tradition in this field of research, the periodic substrate potential of the generalized FK model is assumed to be a sinusoidal curve. Traditionally parabolic approximations [10] of an unsymmetrical double-well potential are used however only for analytical studies for one mesh. We avoid the non-differentiable overlaps of the diverse parabola by a continuously differentiable cosine ansatz with three summands. It is just better. Additionally it allows the treatment of the full chain and not only the study of a single part of the ledge of meshes.

The chain is really assumed of finite length with free boundaries. We search the form of the movement of the FK chain on the site-up potential from a lower minimum of Au to an upper minimum of Ma, for N meshes. We search for a low global valley through the 'mountains' of the N-dimensional PES for steps of the chain along a minimum energy path (MEP). The aim is a step by step movement along the scheme of Fig. 1. However, with a totally symmetric external force, the displacive shear transformation mechanism [11], the pathway will often be somewhere side-up from the MEP. Thus the totally symmetric excitation will not lead to a consecutive phase transition like it is suggested in Fig. 1.

We use a slightly distorted external force, and the ansatz of a Langevin equation with a second-order vibrational part.

In Sect. 2, we introduce the general model of the phase transition, and in Sect.3, we explain the generalized FK model used in this paper with the special case of N=16 chain length. In a next section, we repeat the definition of Newton trajectories (NT) and the use of a Langevin equation (LE). In main Sect. 6, we calculate and discuss the application of both tools. NTs are used to explore the PES and find MEPs, or low paths, con-

[a] e-mail: quapp@math.uni-leipzig.de (corresponding author)
[b] e-mail: jmbofill@ub.edu

Published online: 25 May 2022

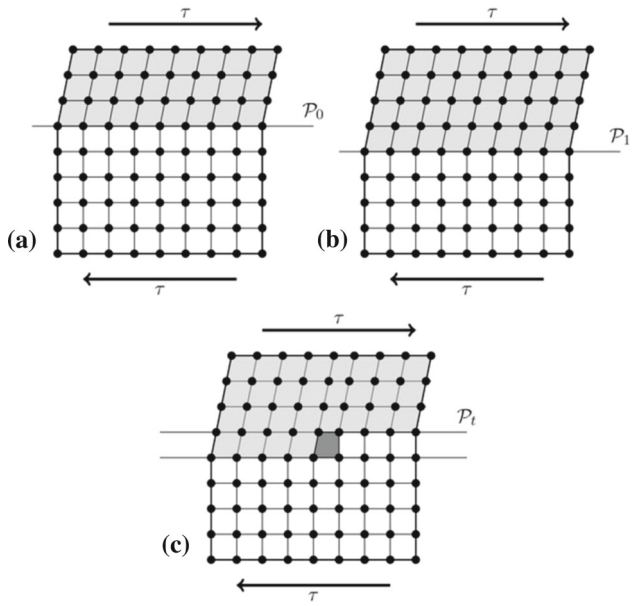

Fig. 1 Model of the lattice with phase boundaries [3]. From **a** to **b** the ledges go one step further. In panel **c** a single mesh is shown at any coordinate x_i. The orthorhombic lattice is Ma, the cubic one is Au. Courtesy Springer Nature

necting minima and SPs of a lower index, like 1 or 2. An LE is used to describe explicitly the Au–Ma phase transition. We find an interesting description of the phase changing process. And it can be got by a simple equation, at all. Finally, the last sections are devoted to a discussion and a conclusion.

2 The model

The model for the Au–Ma phase transition is explained in Ref. [3]. We reproduce Fig. 2 of this paper in Fig. 1. Using the free energy per unit volume of the material one gets a description for every mesh of a one-dimensional lattice (named ledge) by an unsymmetrical double minimum potential [12]. A general explanation of microstructures in cubic to orthorhombic transitions can be found in [1,2,13]. Note that the equal length of the two different meshes for Au and Ma leads to the assumption of equal distances between the Au–Au bonds and the Ma–Ma bonds which in reality is somewhat questionable. The lath spacing between different ledges is also not tractable by our simplification, compare [11,14].

3 The generalized FK model

In general, the vector $\boldsymbol{x} = (x_1, ..., x_N)^T$ represents the ledge of N meshes for a finite N. It holds that $x_i < x_{i+1}$ for $1 \leq i \leq N$. A mesh is a 4-particle piece of the

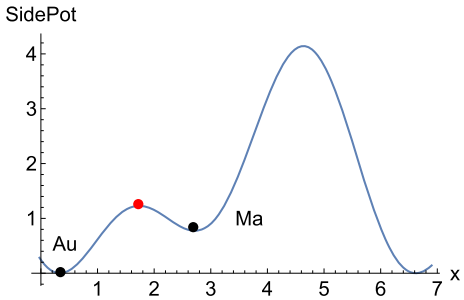

Fig. 2 The site-up potential function which is used for the first mesh x_1. Au is the zero minimum, and Ma is the upper minimum at 0.77 arbitrary units. Both are depicted by black bullets, where the SP in between is a red bullet. Its energy height is 1.23 units. The large peak before the next Au minimum at 2π is a special barrier against general sliding of the ledge

lattice, compare Fig. 1, where we additionally isolate a single ledge of the 2D lattice, and study the change of the relation of the phase of the 4 particles of one mesh from the Au to the Ma structure. The chain has the parameters $a_o = a_s = 2\,\pi$ where a_o is the equilibrium distance of the meshes, x_i, and a_s is the periodicity of the site-up potential of the remaining ledges of the full lattice which is assumed in a generalized FK model. The one ledge of interest is embedded in the full lattice which is the reason for $a_o = a_s$ leading to a simple FK model. We use the parameter k for the 'spring force constant' between the meshes. The parameter regulates the relation between the spring force and the site-up potential. F is the amount of an external force which usually is equally applied to all meshes x_i [3]. (In Fig. 1, it is depicted by τ.) The application of force F is explained in Sect. 5. Note that such an ansatz represents the general case of a shear force, but it makes it difficult to get single steps for the consecutive meshes, as it is depicted by the dark mesh in Fig. 1c.

The meshes x_i are the former 'particles' of the generalized FK model. We treat a simple harmonic spring potential [3]

$$S(\boldsymbol{x}) = \frac{k}{2} \sum_{i=1}^{N-1} (x_{i+1} - x_i - a_o)^2, \tag{1}$$

where k is the spring force constant. The nearest neighbour distance is $a_o = 2\pi$. The nearest neighbour springs can, of course, be adapted to a more realistic relation by a twofold nearest neighbour ansatz, to reflect the Au–Au bond springs, compare Refs. [15–17]. One can also put possible other Ma–Ma bond springs, and one can put the Au–Ma bonds into the overall site-up potential.

The PES for the variable changes of the x_i is the Frenkel–Kontorova model

$$V(\boldsymbol{x}) = P(\boldsymbol{x}) + S(\boldsymbol{x}), \tag{2}$$

where we propose the site-up P with the generalized potential, compare Fig. 2,

$$P(\boldsymbol{x}) = \sum_{i=1}^{N} [-0.1\cos(x_i) \ -\cos(2\,x_i) \\ +1.5\cos(x_i - 4.5) + 1.66]\,. \qquad (3)$$

We use the periodicity $a_s = 2\pi = a_o$ of the cosine function, here and in the spacing of the spring forces. The mesh x_1 has no 'bond' to the left-hand side, and the mesh $x_{16} = x_N$ has no 'bond' to the right hand side, thus the chain has free boundaries. The factors 0.1 at the first part, and 1.5 at the third summand regulate the relation of the two minimum wells. If these factors depend on temperature, one could change the potential in a desired direction. In this paper we do not treat explicitly the temperature. Thus the complicated interplay between stress and temperature of shape memory alloys [14,18] is not directly contained in the model of this paper. Note that the second barrier height to the next mesh must be sufficient to prevent the mesh points to move out of their places. The postulate is essential for the model to work automatically. Any point, x_i, should move between the Au minimum and the Ma minimum only. The full chain should be fixed in this region. In this sense the potential represents a bistable link [19]. To overcome the large barrier would mean the beginning of a crack of the crystal [14,18,20] which is not of interest in this paper.

We search consecutive 'jumps' of the meshes j from their 'zero'-minimum Au to the up-minimum well, Ma, but we will prevent the chain from general sliding. So to say, the Au phase can only 'relax uphill' to the Ma phase in the right direction if the external force drives it. This property is realized for moderate forces by the third part of Eq.(3) making the big peaks of the site-up potential. Vice versa can an inverse force push the Ma phase into the downhill direction to the Au phase.

The generalized potential in Eq. (3) is not the often used parabolic double minimum potential [3,17]. For such parabolas is not described how the high limit between the meshes can be defined. Treating only one mesh with its double minimum [3,21] 'one at a time'—is not enough for the study of a consecutive excitation of neighbouring meshes along the ledge of interest in the given crystal, the full generalized FK model. The potential is also not a piece-wise linear function [19].

In history, in times long ago, the use of two parabolas was introduced for simplicity only [10,17]. We think that consecutive parabolas with no differentiable crossing points of their energy curves [21] are not really a simplification, if one looks for the full ledge. The edge usually causes an nonphysical behaviour. We guess that all atoms of the crystal are hold at their places by chemical bonds. The forming or disruption of bonds is described by a continuous, differentiable potential with a usual SP. (Note that the hand drawn Fig. 1 in [21] does not correctly reflect the used PES by the seemingly differentiable double minimum potential.)

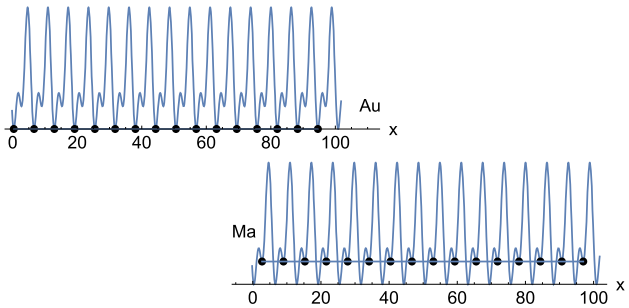

Fig. 3 Two 'global' minima of the crystal for $N = 16$: all x_i at $(2\pi\, i + \delta)$ are sitting equally along a ledge. Here only counts the site-up potential. The spring potential, $\mathrm{S}(\boldsymbol{x})$, is zero. Note that we usually draw the x_i sitting on the site-up potential, beginning with the right panel in this figure, to lead the eye. In the correct model all x_i will be on the axis. Their distances only can change

In Fig. 3 we represent two known 'global' minima of the chain. Their energies are zero for the Au ledge, and 12.39 units for a full ledge of Ma, correspondingly. Per mesh, x_i, there holds the energy difference of 0.77 units. A single transition state is at 1.23 units, see Fig. 2.

4 Newton trajectories

NTs are help tools to study a complicated PES. They explore the pathways between different stationary points, see refs. [6–9,22–28]. We use a force

$$\boldsymbol{f} = F\,(f_1, ..., f_N)^T = F\,(1, ..., 1)^T \qquad (4)$$

where the last setting is the usual unique case of a shear force over all meshes of the ledge. Thus all single components f_i are unique. Sometimes we allow slight deviations from this setting. The superscript T denotes the transpose. The force forms the effective potential energy

$$V_{eff}(\boldsymbol{x}) = V(\boldsymbol{x}) - \boldsymbol{x}^T\,\boldsymbol{f}, \qquad (5)$$

where $V(\boldsymbol{x})$ is the original PES (2). The external force will result in a distortion of the original minima and saddle points (SPs). The new stationary points on the effective potential satisfy the condition $\nabla_{\boldsymbol{x}}\ V_{eff}(\boldsymbol{x}) = \boldsymbol{0}$, which implies

$$\nabla_x\ V_{eff}(\boldsymbol{x}) = \boldsymbol{g}(\boldsymbol{x}) - \boldsymbol{f} = \boldsymbol{0}. \qquad (6)$$

This means that in the new set of stationary points of $V_{eff}(\boldsymbol{x})$, the gradient of the original PES, $\boldsymbol{g}(\boldsymbol{x})$, has to be equal to the external force, $\boldsymbol{f}$. For a properly chosen force direction, the energy of a minimum is increased, and the energy of a neighboured SP is lowered [29]. Solution points for different amounts of F of Eq. (6) form a curve which is named Newton trajectory. A general direction $(f_1, ..., f_N)$ is named the search direction

of the NT. Every NT describes a connection between different stationary points of an index difference of one [30]. Following an NT numerically is a method to search a next SP if a minimum is given, or vice versa.

5 Dissipative Langevin equation (LE)

We assume an external force to form an effective potential by Eq. (5). In many shape memory alloys one has a stress induced Ma [11]. We search this transition here along a trajectory $\boldsymbol{x}(t)$. We use the spring force with $k = 1$. The usual vibrations of the meshes have to be taken into account. We introduce for the calculation of the second-order equation the vector function $\boldsymbol{v}(\boldsymbol{x}) = \boldsymbol{x}'$ for the velocity of the meshes. Nodes on an LE trajectory are calculated numerically. Starting at an original Au minimum of $V(\boldsymbol{x})$, we put the numerical solution forward by the steps along the system of dimension $2\,N$

$$\Delta x_i(J+1) = \epsilon v_i(J)\ , \tag{7}$$

$$\Delta v_i(J+1) = -\frac{\epsilon}{m}(\eta\ v_i(J) + \mathrm{grad}_i(J) - F\,f_i) \tag{8}$$

for $i = 1, ..., N$. The counter J stays for the 'nodes' of the trajectory, ϵ is the scaling of the step length of the LE, thus a time step, m is the mass of a mesh, here used with $m = 1$, and $grad_i$ is the derivation of the potential (2) to coordinate x_i at node J. The component $F\,f_i$ remains of the effective potential (5) after differentiation. By the constant η we can regulate the degree of damping. We use the value of $\eta = 0.05$ for a small friction.

The components of the gradient of the effective PES are

$$\begin{aligned}\mathrm{grad}_{eff\,i} &= \mathrm{grad}_i - F\,f_i \\ &= k\,(x_{i+1} + x_{i-1} - 2\,x_i) + P_{x_i} - F\,f_i\end{aligned} \tag{9}$$

for $i = 2, ..., N-1$. For $i = 1$ and $i = N$ emerge the boundary components

$$\begin{aligned}\mathrm{grad}_{eff\,1} &= \mathrm{grad}_1 - F\,f_1 \\ &= -k\,(x_2 - x_1 - a_o) + P_{x_1} - F\,f_1\ , \end{aligned} \tag{10}$$

$$\begin{aligned}\mathrm{grad}_{eff\,N} &= \mathrm{grad}_N - F\,f_N \\ &= k\,(x_N - x_{N-1} - a_o) + P_{x_N} - F\,f_N.\end{aligned} \tag{11}$$

The system of Eqs. (7)/(8) is a coupled nonlinear system because of the coupled gradient parts, and the nonlinear part of the derivatives, P_{x_i}. Numerically we approximate solutions of Eqs. (7)/(8) with ϵ-steps of length 0.0025. In the representation we depict the J-axis by 'Node'.

If one starts the LE at a minimum of $V(\boldsymbol{x})$ with a small force, $\boldsymbol{f}$, then the chain will stay in its bowl. Any vibration will take place here. But if one chooses $F > F_c$, a critical force, then the Langevin equation with external force will lead to a possible change of the chain over an SP. By a stronger force an Au minimum will be depinned and the mesh slides 'downhill' the effective PES to an Ma minimum.

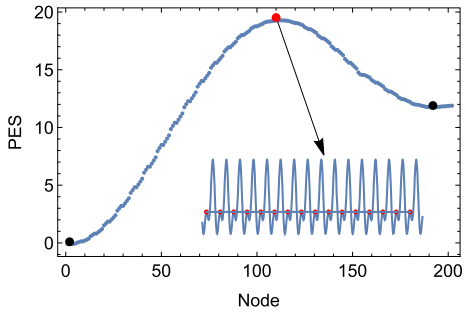

Fig. 4 Energy profile over the 'trivial' NT starting in the zero minimum of the Au ledge and going uphill totally symmetrically over all SPs at the same time—the trivial solution. The inset is an SP of index 9. The up-minimum is the full Ma-structure of all meshes. Black bullets are minima, the red bullet is the 'global' SP. Its energy is N times the energy of the single SP of Fig. 2

The movement under the unique excitation $F\,(1, .., 1)^T$ usually leaves the chain structure unchanged. The full chain moves like a fixed body along the side-up potential. This pathway is named 'trivial' and it is quite stable for an overdamped LE with a large η.

For other applications of a Langevin equation see refs. [9,31,32].

6 Results

6.1 Results for Newton trajectories

We present different cases for NTs for an uphill pathway from the global Au minimum to the full Ma minimum. The search direction for the NT is the vector of units of the form $(1, ..., 1)^T$, in the fully symmetric case, in Fig. 4, named the trivial solution. To find a nontrivial solution, we use a slight asymmetric push: we set the first component to $f_1 = 1.05$, and all other $f_j = 1$, see Fig. 5. In contrast, for a slight asymmetric pull we set the last component to $f_N = 1.05$, where the energy profile looks equally to the former case, and for a combined kink and antikink starting in the centre of the meshes, we set the 8th component $f_8 = 1.05$, see Fig. 6.

The figures are drawn over the steps of the NTs, named nodes. The step length in the 16-dimensional coordinate space of the meshes is 0.05. In Fig. 4 all parts of the chain move equally pushed by the unique forces for all meshes. Here no deformation of the ledge takes place, see the Appendix. All distances will be fixed by $2\,\pi$. The chain thus is going over a 'global' fully symmetric ridge uphill to the 'global' SP of index 9 with an energy of 19.65 units where all meshes are on their own

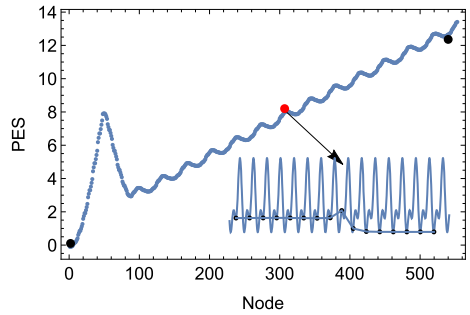

Fig. 5 Energy profile over an NT starting in the zero minimum and going uphill slightly unsymmetrically, with $f_1 = 1.05$ but all other $f_j = 1$. It 'pushes' the left part of the chain a little bit more. After a symmetric start, it finds back to the single SPs of the Ma meshes in a consecutive kind, and passes the single minima of the single Ma wells. The inlet shows the SP of the 9th mesh. At the end, the up-minimum is again the full Ma-structure of all meshes, see the right structure in Fig. 3

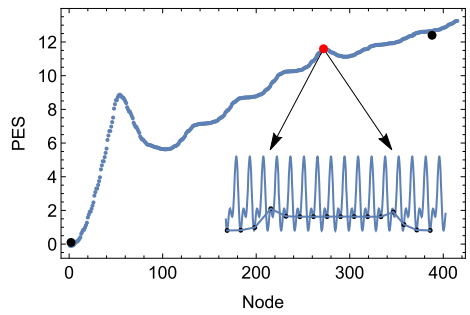

Fig. 6 Energy profile over an NT starting in the zero minimum and going uphill slightly unsymmetrically, with $f_8 = 1.05$. It 'pulls and pushes' the centre of the chain a little bit more. After a symmetric start, it comes back to the single SPs of the Ma meshes from the centre, and goes in a twofold kind to the boundaries. It finds consecutively two single minima of two single Ma wells. At the end, the up-minimum is again the full Ma-structure of all meshes

single SP, compare the red bullets of Figs. 2 and 4. The 'global' SP is the combination of all single SPs of all meshes in their corresponding dimensions [33–35]. The index 9 includes one (maximally negative) eigenvalue to the eigenvector of a unique direction of all meshes, and asymmetric vibrations. The 'trivial' NT follows the first eigenvector.

There are animation files of Figs. 5 and 6 in the SI part.

Figure 5 shows the energy profile of the PES (2) over an NT. It starts for ≈ 50 nodes with a symmetric excitation of all meshes, so to say it starts with the beginning of the trivial solution. However, then the NT turns down and forms a sketch of the MEP over all single SPs of index 1 between the two 'global' minima of Fig. 3. The search direction for the NT is the vector $(1.05, 1, , ..., 1)^T$. The fully symmetric NT of Fig. 4 has a bifurcation point on the ridge. The small distortion by f_1 here causes a near neighbouring NT which deviates from the symmetry before the bifurcation point [22,23]. Because NTs connect stationary points, this NT then finds the SP of index 1 of the next single mesh transition. And so on. One can observe the corresponding single SP_i and the next intermediate minima, iMin_i of consecutive meshes, compare the inset of Fig. 5. The structure of the minima of all x_i up to $N-1$ is a shock. (In the FK community it is named antikink, a compressed structure.) Compare Fig. 1: all left points already are near the Ma minimum, then one has a shorter Ma–Au distance, a shock, and all remaining points are still below near the Au minima.

The step-like pathway has its ground in the mutual springs of the meshes by Eq. (1) where we used $k = 1$. Not only the site-up potential counts, but also the 'springs' between the meshes. The consecutive steps from i to $i+1$ look like a travelling wave [6–9], see the SI animations. The pathway of Fig. 5 after node ≈ 100 corresponds to the imagination of Fig. 1c.

In Fig. 6, the energy profile for an NT is depicted where the mesh x_8 is a little bit more excited by $f_8 = 1.05$, instead of 1 only, like the other force components. It is known that an ultra low load at an intender of Au can trigger a Ma transition [36,37]. Here the 'wave' of excitations starts at the centre of the chain, at x_8, and a kink goes to the left, but an antikink goes to the right hand side. Consequently, only 16/2 combined SPs are to overcome, because always two single SPs are crossed at the same NT step.

Note that NTs are only artificial curves to explore the PES of a problem. The trajectories are usually not mechanical trajectories of a moving system. Thus we discuss a more physical ansatz in the next subsection.

6.2 Results for a Langevin equation (LE)

We get a (somewhat smeared) consecutive excitation of the Au phase transition along a ledge, to the Ma phase. Using a small value for the damping $\eta = 0.05$, we excite the chain by a moderate external force

$$\boldsymbol{f} = 4\ (1.1, 1, ..., 1, 1.1)^T\ . \tag{12}$$

At the left and the right border we use a slightly higher excitation to avoid a fully symmetric excitation of the chain. We approximate solutions of Eqs.(7) / (8) numerically with ϵ-steps of length 0.0025. Figures 7 and 8 show a result. The energy profile on the original PES (without the external force) first shows a vibration of the chain in its Au bowl, up to node 33 000. Then it nicely climbs up to Ma under vibrations. This is illustrated by the structures of Fig. 8. The right structure of Fig. 8 is a quasi perfect Ma chain though the chain executes further vibrations. The structures at the left-hand side of Fig. 8, and in the centre show how the meshes from the left and the right hand sides climb step by step uphill over their single SPs. At the end, at node 82 800, the central meshes are also lifted to Ma.

In a second example we treat a chain of 47 meshes, thus we use 47× the potential of Fig. 2. Again we start

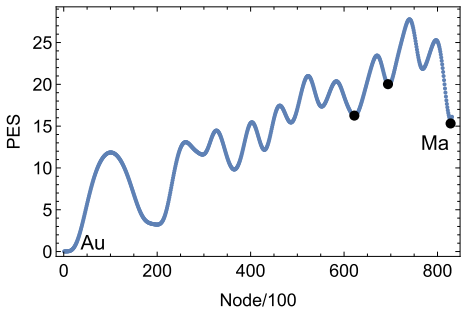

Fig. 7 Energy profile over the original PES of a solution for the LE with vibration term, between global low-minimum and up-minimum. The force is given in Eq. (12) by 'pushes'. After a vibration of the chain in its bowl, we get a successive increase up to the Ma level. The black bullets are shown in Fig. 8

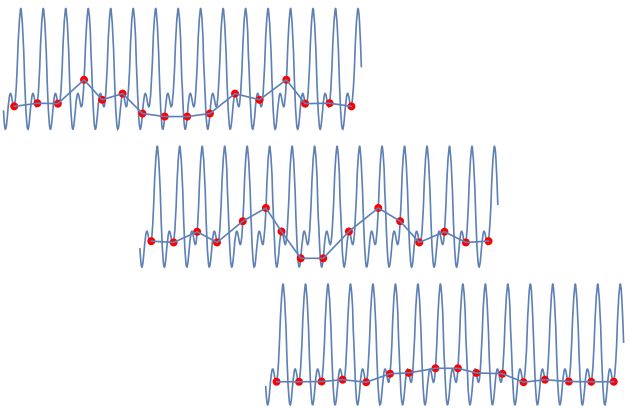

Fig. 8 Structure of the chain for the three black bullets in Fig. 7. Successively the chain claims uphill to the Ma structure, but under some symmetric vibrations of different parts

with an unsymmetry at the left-hand side by force component $f_1 = 1.1$, but all other components equal to one. The amount of the force is balanced to $F = 6.75$ units. The force is far below the trivial symmetric SP, but still enough to depinn one mesh after the other of the chain from the Au minimum. In Fig. 9 we show an energy profile of a Langevin solution (only every 25th node is shown). The four first, or so, peaks are vibrations of the full chain in the site-up minima of Au. However, then starts the successive rise to single Ma minima. Vibrations of the single meshes around their equilibrium minima take place in the last region of the profile. In Fig. 10 we show the final structure of the chain in this calculation at node 65 000. In SI we also represent an animation of the solution.

7 Discussion

We propose a continuously differentiable potential of the Au to Ma transformation problem, in contrast to many former workers. The ansatz by a Frenkel–Kontorova model allows a complete treatment of a full ledge of meshes in one calculation for a Langevin equation. Of course, every calculation of a ledge needs a finite chain with given fixed or free boundaries, in contrast to refs. [15–17].

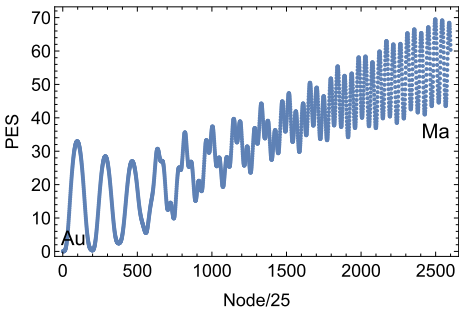

Fig. 9 Energy profile of the 47-dimensional PES only of a solution for the LE, between global low-minimum and up-minimum. The force pushes the chain to Ma. After a vibration of the chain in their bowl, we get a successive increase up to the Ma level

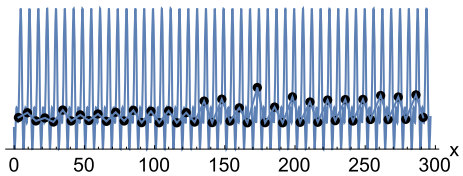

Fig. 10 Structure of the final chain of a Langevin calculation in the 47D case. The chain has claimed uphill to the Ma structure. Some (nonsymmetric) vibrations of different parts still happen

There are many former papers which treat only one mesh of the ledge. To calculate for one index i the movement only, so to say alone for the single potential of Fig. 2, is not enough. One needs the view over all the meshes of a ledge in Fig. 1, in one common system of equations. The springs, $\mathbf{S}$, of the FK model, Eq. (1), realize the connection. By the gradients, Eqs. (10), this system is a coupled system. And as recently as the coupling represents the problem of the treated transition from Au to Ma in an alloy.

The usually given external force is a vector of equal components for all meshes. However, one has to leave the full symmetry, at least by a small perturbation. For our 'toy'-problem with $N = 16$ meshes, the symmetric TS is only a little bit higher than consecutive single SPs. This will not hold for a larger alloy. The symmetric barrier height goes with $N*($ barrier of one $SP_1)$, which we should avoid. Thus, some small deviations in the force vector, $\boldsymbol{f}$, can lead to much lower barrier heights if one excites the chain of meshes one after the other. A nice result for such a case is shown in Fig. 8. Note that qualitatively are the cases equal, the small case with $N = 16$ and the medium case with $N = 47$ meshes.

8 Conclusion

Doing some simple numerical experiments, we find a mixed picture of excitations of one or more meshes of the ledge which forms the proposed generalized FK model. Usually unique stress by a shear force over the full ledge does not lead to consecutive transformations of single meshes, like Fig. 1 suggests it; however, this is possible in special cases. Nice consecutive excitations to Ma states can start at the boundaries of the ledge, or anywhere inside the chain, if a slightly distorted shear force is assumed.

If in a practical case the alloy of interest is much larger than the toy cases of $N = 16$ or 47 meshes, as they are used here for our explanations, then we can assume that small perturbations of any kind destroy a given symmetry of a unique shear force. Then a pathway much lower than the trivial, the symmetric ridge path over all N meshes will emerge simultaneously.

Acknowledgements The authors thank for the financial support from the Spanish Ministerio de Economía y Competitividad, Projects No. PID2019-109518GB-I00, PID2020-1 CTQ2017-87773-P/AEI/ FEDER, and the Spanish Structures of Excellence María de Maeztu program through grant MDM-2017-0767.

Author contributions

All authors contributed equally to the paper.

Funding Open Access funding enabled and organized by Projekt DEAL.

Availability of data Data of all states and pathways reported in the paper are available on request by WQ. This manuscript has data included as electronic supplementary material. The online version of this article contains supplementary material, which is available to authorized users.

Declarations

Conflict of interest We disclose financial or non-financial interests that are directly or indirectly related to the work. (Of course, we declare scientific interests.)

A Appendix

A translation symmetric force does not change the spring potential. We use $\mathbf{1} = (1_1, \ldots, 1_N)^T$. Multiplying the derivative of the spring potential from the left by $\mathbf{1}^T$ we obtain the sum of the scalar product $\mathbf{1}^T \nabla_{\boldsymbol{x}} S(\boldsymbol{x})$. The set of partial derivatives of $S(\boldsymbol{x})$ (see Eq. (1)) with respect to x_i for $i = 1, \ldots, N$ is

$$\frac{\partial S(\boldsymbol{x})}{\partial x_1} = -k(x_2 - x_1 - a_0) = -k(\Delta x_1 - a_0)$$

$$\frac{\partial S(\boldsymbol{x})}{\partial x_2} = k(x_2 - x_1 - a_0) - k(x_3 - x_2 - a_0) = -k(\Delta x_2 - \Delta x_1)$$

$$\frac{\partial S(\boldsymbol{x})}{\partial x_3} = k(x_3 - x_2 - a_0) - k(x_4 - x_3 - a_0) = -k(\Delta x_3 - \Delta x_2)$$

$$\vdots$$

$$\frac{\partial S(\boldsymbol{x})}{\partial x_{N-1}} = k(x_{N-1} - x_{N-2} - a_0) - k(x_N - x_{N-1} - a_0) = -k(\Delta x_{N-1} - \Delta x_{N-2})$$

$$\frac{\partial S(\boldsymbol{x})}{\partial x_N} = k(x_N - x_{N-1} - a_0) = k(\Delta x_{N-1} - a_0),$$

where $\Delta x_i = x_{i+1} - x_i \ , \quad i = 1, \ldots, N-1$. Summing all these expressions we have that $\mathbf{1}^T \nabla_{\boldsymbol{x}} S(\boldsymbol{x}) = 0$. This means that $\nabla_{\boldsymbol{x}} S(\boldsymbol{x})$ is orthogonal to $\boldsymbol{f} = F\mathbf{1}$.

Supplementary Information (SI)

We add some movies as it is described in the text above. They can be studied by the programme 'gwenview' under Linux. The movies are made by the Mathematica program.

– Excitation of the chain more left by f_1=1.05 (push) by FKmAnimMeshPush.gif

– Excitation more right by f_{16}=1.05 (pull) which is not shown here by a figure FKmAnimMeshPull.gif

– Excitation more at the centre by a push-pull for f_8=1.05 FKmAnimMeshcenterNT.gif

– Dynamical Langevin 16 meshes FKmAnimMeshLangIIvib.gif

– Dynamical Langevin 47 meshes FKmAnimMeshD47.gif

References

1. J.A. Shaw, S. Kyriakides, Acta Mater. **45**, 683 (1997)
2. N.J. Bechle, S. Kyriakides, Int. J. Solids Struct. **51**, 967 (2014)
3. P. Leninpandian, S. Vedantam, Ann. Solid Struct. Mech. **12**, 89 (2020)
4. T.A. Kontorova, Y.I. Frenkel, Zh. Eksp, Teor. Fis. **8**, 89 (1938)
5. M. Marder, S. Gross, J. Mech. Phys. Solids **43**, 1 (1995)
6. W. Quapp, J.M. Bofill, Mol. Phys. **117**, 1541 (2019)
7. W. Quapp, J.M. Bofill, Eur. Phys. J. B **92**, 95 (2019)
8. W. Quapp, J.M. Bofill, Eur. Phys. J. B **92**, 193 (2019)

9. W. Quapp, J.Y. Lin, J.M. Bofill, Eur. Phys. J. B **93**, 227 (2020)
10. W. Atkinson, N. Caberra, Phys. Rev. **138**, 763 (1965)
11. J.F. Xiao, X.K. Shang, J.H. Hou, Y. Li, B.B. He, J. Plast. **146**, 103103 (2021)
12. B.L. Sharma, J. Mech. Phys. Solids **96**, 88 (2016)
13. K.F. Hane, T.W. Shield, J. Elast. **59**, 267 (2000)
14. P. Shayanfard, E. Alarcon, M. Barati, M.J. Mahtabi, M. Kadkhodaei, S.A. Chirani, P. Sandera, Crit. Rev. Solid State Mat. Sci (2021)
15. L. Truskinovsky, A. Vainchtein, Phys. Rev. B **67**, 172103 (2003)
16. L. Truskinovsky, A. Vainchtein, SIAM J. Appl. Math. **66**, 533 (2005)
17. E. Trofimov, A. Vainchtein, Contin. Mech. Thermodyn. **22**, 317 (2010)
18. E. Sgambitterra, P. Magaro, F. Niccoli, F. Furgiuele, C. Maletta, Shape Mem. Superelast. **7**, 250 (2021)
19. A. Cherkaev, E. Cherkaev, L. Slepyan, J. Mech. Phys. Solids **53**, 407 (2005)
20. N. Shafaghi, B. Haghgouyan, C.C.C. Aydiner, G. Anlas, Mater. Today Proc. **2**, 763 (2015)
21. L. Wang, R. Abeyaratne, J. Mech. Phys. Solids **116**, 334 (2018)
22. W. Quapp, M. Hirsch, O. Imig, D. Heidrich, J. Comput. Chem. **19**, 1087 (1998)
23. W. Quapp, M. Hirsch, D. Heidrich, Theor. Chem. Acc. **100**, 285 (1998)
24. J.M. Bofill, J.M. Anglada, Theor. Chem. Acc. **105**, 463 (2001)
25. R. Crehuet, J.M. Bofill, J.M. Anglada, Theor. Chem. Acc. **107**, 130 (2002)
26. W. Quapp, J. Theoret. Comput. Chem. **2**, 385 (2003)
27. W. Quapp, J.M. Bofill, Theoret. Chem. Acc. **135**, 113 (2016)
28. W. Quapp, J.M. Bofill, J. Ribas-Ariño, J. Phys. Chem. A **121**, 2820 (2017)
29. L. Pauling, Chem. Eng. News **24**, 1375 (1946)
30. M. Hirsch, W. Quapp, J. Mol. Struct. THEOCHEM **683**, 1 (2004)
31. W. Quapp, J.M. Bofill, Eur. Phys. J. B **94**, 66 (2021)
32. W. Quapp, J.M. Bofill, Eur. Phys. J. B **94**, 64 (2021)
33. D. Heidrich, W. Quapp, Theor. Chim. Acta **70**, 89 (1986)
34. R.M. Minyaev, I.V. Getmanskii, W. Quapp, Russ. J. Phys. Chem. **78**, 1494 (2004)
35. P. Collins, G.S. Ezra, S. Wiggins, J. Chem. Phys **134**, 244105 (2011)
36. B.B. He, M.X. Huang, Z.Y. Liang, A.H.W. Ngan, H.W. Luo, J. Shi, W.Q. Cao, H. Dong, Scr. Mater. **69**, 215 (2013)
37. B.B. He, X.K. Shang, Philos. Mag. Lett. **101**, 417 (2021)